Wave Motion 77 (2018) 139–155

Contents lists available at ScienceDirect

Wave Motion

journal homepage: www.elsevier.com/locate/wamot

Wave-based vibration control of large cable net structures

Yang Liu, Kai Zhang *, Wei-Zhong Zhang *, Xiu-Yun Meng

School of Aerospace Engineering, Beijing Institute of Technology, Beijing, 100081, China

HIGHLIGHTS

- A wave-based boundary control strategy on the large cable net structure is proposed.
- Stability results are given with disturbances coming from the external boundary.
- Dynamic responses of a planar cable net structure are numerically analyzed.
- Structural vibration can be controlled effectively by applying our proposed strategy.

ARTICLE INFO

Article history:
Received 18 March 2017
Received in revised form 29 October 2017
Accepted 13 November 2017
Available online 22 November 2017

Keywords:
Cable net structure
Wave-absorbing control
Vibration control
Irrational transfer function

ABSTRACT

Large cable net structures have been widely applied in aerospace engineering due to the feature of light-weight, high packaging efficiency, and high thermal stability. Structural vibrations induced by a variety of disturbances are inevitable in the space environment, resulting in the requirement of effective vibration control strategies for large cable net structures. Since the large cable net structures have many closely spaced vibrational modes in the range of low frequencies, traditional modal based control may cause modal truncation and spillover problems. In this paper, a wave-based boundary control strategy is adopted and its effectiveness to control the vibration of cable net structures is investigated, by transfer function analysis and numerical methods. It is found that the structural vibration can be absolutely resisted by applying the wave-based boundary controllers onto all the exterior nodes, when disturbances come from the external boundaries of the cable net. Our results in this paper can provide a theoretical basis for the vibration control of large cable net structures.

1. Introduction

Large cable net structures, known as a type of flexible structures, can be easily packaged in a small volume and provide high stiffness when stretched. Besides, cable net structures possess the features of light-weight and high thermal stability, resulting in wide applications in aerospace engineering. For example, the AstroMesh reflector family, fabricated by the Northrop Grumman Corporation, has been used in many renowned projects such as Thuraya, INMARSAT 4, and MBSAT, c.f. [1]. During the usage in the space environment, structural vibrations would be caused by a variety of disturbances, including alternating thermal loads, attitude maneuvers of the spacecraft and impact from space debris [2]. However, the damping of the cable net structures is such low that the introduced vibrations are hard to decay, which will influence the surface accuracy of the reflectors severely. Hence, an efficient vibration control strategy on large cable net structures is required.

* Corresponding authors.
E-mail addresses: zhangkai@bit.edu.cn (K. Zhang), hellowezwz@bit.edu.cn (W.-Z. Zhang).

https://doi.org/10.1016/j.wavemoti.2017.11.004
0165-2125/

The vibration control of flexible structures can be implemented by active or passive methods. However, passive methods can be sensitive to resonance frequencies, may be bulky, and may not perform well at low frequencies [3]. In comparison, active methods have the potential to overcome the performance limitations of passive methods [4,5]. The most widely used method for active vibration control of flexible structures is based on modal control theory, where the structural dynamic responses are considered as the superposition of all vibrational modes [6–9]. Modal-based active vibration control methods try to attenuate the amplitudes of the modal displacement, and the number of considered vibration modes must be determined before the controller design. With the increasing scale of the cable net structure, close modes of the flexible structure exist in the range of low frequencies [10], making it hard to deal with the modal truncation problem. In addition, dynamic responses of a large flexible structure do not immediately spread to the entire structure under an impact or a disturbance, but in a gradual manner of wave propagation [2]. Consequently, the modal control methods are generally ineffective.

A wave-based theory is proposed to control the vibration of large space structures by Von Flotow et al. [11], where the structural elastic dynamic responses are regarded as the superposition of two traveling waves along opposite directions. Quite a few wave-based active control methods, such as traveling wave control [11], wave-absorbing control [12], active sink method [13], have been proposed since 1986. These active control strategies try to stop the formation of vibrations by wave cancellation. Since the controllers are designed directly based on wave equations, the wave-based methods have shown the abilities to avoid high-frequency spill and modal truncation comparing with the traditional modal control methods [14].

Boundary control has the ability to remove the spillover problem since the control is proposed on the base of the original distributed-parameter systems [15], whose boundary affects all the flexible modes [16]. The wave-based boundary control method has shown great power and simplicity in the vibration control of flexible structures. In Ref. [17], the actuator is located at one end of the structure of the beam-like mass–spring arrays to control its planar position while absorbing the vibration by canceling the outgoing waves. In Ref. [18], the torsional vibrations in drill strings are controlled by decomposing the drill string dynamics into two traveling waves and absorbing the wave traveling in the direction of the top drive. In Ref. [19], the flexural vibration of a slender structure is controlled by the use of an adaptive anechoic termination, which is fulfilled by applying force determined by a feed-forward adaptive control that uses estimates of the incident and reflected waves as reference and error signals. Unfortunately, the wave-based boundary control method on large cable net structures still lacks. This motivates us to find a new vibration control strategy for cable net structures.

In a real cable network antenna reflector, the cable ends are fixed at the ring truss, which is connected to the satellite by a deployable mast. Disturbances are most frequently generated during attitude maneuver or orbit transfer and then transmitted into the cable net from the boundary truss. Thus, in this paper, disturbances are assumed to come from the external boundaries of the cable net. We adopt a wave-based boundary control strategy and its effectiveness to control the vibration of space cable net structures is investigated. The paper is organized as follows. Section 2 presents the motion equations of a planar cable net structure and gives the wave-based boundary control strategy. In Section 3, transfer functions from the disturbance to the displacement of the cables are derived and pole analysis is given to express the stability results of the wave-based boundary control strategy. In Section 4, the Lax–Friedrichs scheme is adopted to analyze the out-of-plane vibration of the cable net structures and numerical simulations are carried out to show the effectiveness of the wave-based boundary control strategy. Finally, the conclusions are made.

2. Problem formulation

2.1. Model descriptions and assumptions

To simplify the study on the proposed wave-based vibration control methods of cable nets, we consider a planar cable net structure with rigid supports, consisting of triangle-faceted mesh in a periodic pattern, as shown in Fig. 1. Note that the network has only one cable at each boundary point since we adopt the boundary control strategy which applies to the end of each boundary cable. The planar cable net structure can be described by a directed graph $\mathcal{G}$ with its edges denoted by $\mathcal{E} = \{\mathbf{e}_1, \mathbf{e}_2, \ldots, \mathbf{e}_{30}\}$, vertices denoted by $\mathcal{V} = \{\mathbf{v}_1, \mathbf{v}_2, \ldots, \mathbf{v}_{25}\}$, and edge orientations illustrated in Fig. 1. We denote $\mathcal{V}_{int}$ and $\mathcal{V}_{ext}$ as the sets of interior and exterior nodes, respectively. Seen from Fig. 1, $\mathcal{V}_{int} = \{\mathbf{v}_1, \ldots, \mathbf{v}_7\}$, $\mathcal{V}_{ext} = \{\mathbf{v}_8, \ldots, \mathbf{v}_{25}\}$. Similarly, $\mathcal{E}_{int}$ and $\mathcal{E}_{ext}$ denote the sets of interior and exterior edges, respectively, where $\mathcal{E}_{int} = \{\mathbf{e}_1, \ldots, \mathbf{e}_{12}\}$, $\mathcal{E}_{ext} = \{\mathbf{e}_{13}, \ldots, \mathbf{e}_{30}\}$.

Some assumptions are first made for the planar cable net structure. All the cables are assumed undamped and the effect of gravity on the structural response is ignored, due to the space environment. We also adopt the same assumptions as Ref. [20]. In order to ensure a high surface accuracy of the reflector, the cables are usually highly pre-stressed to avoid cable slackening after the antenna is deployed. The high pre-tensioning cable nets are considered as weakly nonlinear systems comparing with single cable [14,21]. Giaccu et al. [22] give a malfunctioning measure to evaluate the deviation from a linear behavior of in-plane cable networks in the absence of slackening effect. It is indicated in that reference that for a given vibration amplitude, the minimum pre-tensioning force can ensure the linear dynamic behavior of the cable network. Thus, the planar cable net can be regarded as linear systems under the vibrations with small amplitude and modal coupling between in-plane and out-of-plane vibrational modes is therefore neglected. In the high pre-tensioning cable net, each cable element is in a taut state. Hook's law of the materials in the cable is valid for the linear system with small amplitude. It is pointed out in Ref. [23] that cable flexural stiffness does not greatly affect the response of a taut cable. We therefore consider the taut cable as the string with constant parameters in this study. In addition, the cable ends of a reflector can be

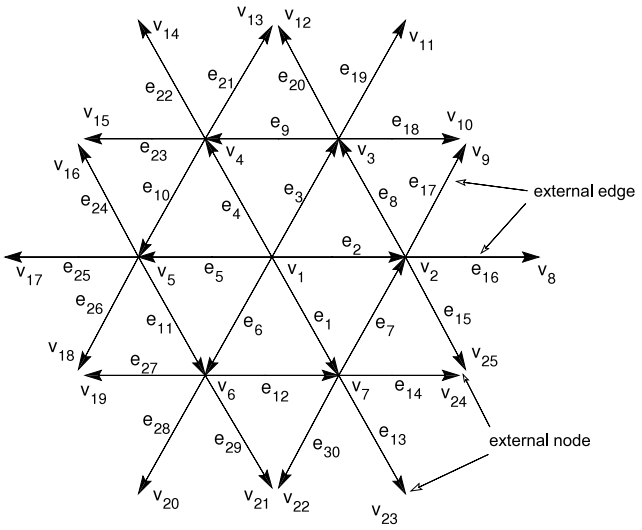

Fig. 1. Schematic of a planar cable net structure with numbered nodes and edges.

considered to be fixed. As a result, the out-of-plane modes dominate in the low-frequency range and the in-plane modes can be neglected in that range [6,24]. The concentrated mass at the junctions may decrease the modal frequencies of a cable network structure as pointed out in Ref. [25]. However, similarly to the previous studies on the vibration control of space cable network structures [6,7,14,26], in order to simplify our object, we also neglect the effect of mass on the vibration in space cable net structures. We first provide the motion equations of the cable net structure governed by the wave equations, then show the control strategy based on wave theory.

2.2. Motion equations

The linear one-dimensional wave equation for each taut string in the cable net structure is

$$T_k \frac{\partial^2 w^k(t,x)}{\partial x^2} - \rho_k \frac{\partial^2 w^k(t,x)}{\partial t^2} = f_e^k(t,x), \quad x \in (0, L_k), t \in \mathbb{R}^+, \tag{1}$$

where $k = 1, 2, \ldots, 30$ means the numbers of the strings (also indices of the edges as shown in Fig. 1). $w^k(t,x)$ represents the transversal displacement of the kth string (edge $\mathbf{e}_k$). t is the time and x means the local coordinate along the kth string. The positive direction of x corresponding to each string is illustrated by the arrows in Fig. 1, so that $x = 0$ corresponds to the start and $x = L_k$ corresponds to the end of each string. T_k, L_k, and ρ_k represent the generic tension, the length, and the linear density of the kth string, respectively. $f_e^k(t,x)$ is the out-of-plane disturbance force applied to the kth string. In the following, $f_e^k(t,x) = 0$ for $k = 1, \ldots, 12$, since we investigate the vibration control of the cable net structure when disturbances come from the external boundary cables. $\mathbb{R}^+$ denotes the set of all positive real numbers.

Let $x = L_k\tilde{x}$ and denote $w_k(t, L_k\tilde{x}) = \tilde{w}_k(t,\tilde{x})$, then Eq. (1) can be normalized to [27]

$$\tilde{c}_k^2 \frac{\partial^2 \tilde{w}^k(t,\tilde{x})}{\partial \tilde{x}^2} - \frac{\partial^2 \tilde{w}^k(t,\tilde{x})}{\partial t^2} = \tilde{f}_e^k(t,x), \quad \tilde{x} \in (0,1), t \in \mathbb{R}^+, \tag{2}$$

where $\tilde{c}_k = (\tilde{T}_k/\tilde{\rho}_k)^{1/2}$ is the normalized wave velocity, and $\tilde{T}_k = T_k/L_k$, $\tilde{\rho}_k = L_k\rho_k$ are the normalized tension and linear density. $\tilde{f}_e^k(t,x) = f_e^k(t,x)/\rho_k$.

In the following, we assume the length of all the edges of the graph $\mathcal{G}$ is 1, i.e. the governing wave equations are normalized, where the tilde symbols in the parameters are removed. So the motion of each string in the entire cable net structure is governed by

$$c_k^2 w_{xx}^k(t,x) - w_{tt}^k(t,x) = f_e^k(t,x), \quad \text{in } \mathbb{R}^+ \times (0,1), \tag{3}$$

where the subscripts t and x refer to the partial derivatives of $w^k(t,x)$ with respect to time and space, respectively.

The equations at all of the internal nodes should meet continuity conditions of displacement and equilibrium conditions, while the equations at the exterior nodes should meet the boundary conditions.

For the central node $\mathbf{v}_1$, the continuity condition of displacement is

$$w^i(t,0) = w^j(t,0), \quad \forall i, j \in I_{\mathbf{v}_1}, t \in \mathbb{R}^+ \tag{4}$$

and the equilibrium condition is

$$\sum_{i\in I_{\mathbf{v}_1}} T_k w_x^i(t,0)=0,\quad t\in\mathbb{R}^+, \tag{5}$$

where i, j mean the numbers of the interior strings, $I_{\mathbf{v}_1}$ denotes the set of numbers of the strings adjacent to node $\mathbf{v}_1$, and $I_{\mathbf{v}_1}=\{1,2,3,4,5,6\}$.

For internal node $\mathbf{v}_i$, $i=2,\ldots,7$, the continuity condition of displacement is

$$w^{i_1}(t,1)=w^{i_2}(t,1)=w^{i_3}(t,0)=w^{i_4}(t,0)=w^{i_5}(t,0)=w^{i_6}(t,0) \tag{6}$$

and the equilibrium condition is

$$T_{i_1}w_x^{i_1}(t,1)+T_{i_2}w_x^{i_2}(t,1)-T_{i_3}w_x^{i_3}(t,0)-T_{i_4}w_x^{i_4}(t,0)-T_{i_5}w_x^{i_5}(t,0)-T_{i_6}w_x^{i_6}(t,0)=0,\quad t\in\mathbb{R}^+, \tag{7}$$

where $(i_1,i_2,\ldots,i_6)$ is the set of numbers of the strings adjacent to node $\mathbf{v}_i$, $i=2,\ldots,7$, $(i_1,i_2,\ldots,i_6)\in\{(2,7,15,16,17,8),(3,8,18,19,20,9),(4,9,21,22,23,10),(5,10,24,25,26,11),(6,11,27,28,29,12),(1,12,30,13,14,7)\}$.

Neumann boundary conditions, namely, the normal derivative of displacement solutions are taken on the boundary of the domains, are applied at all the exterior nodes and can be described as

$$T_r w_x^r(t,1)=u^r(t)+f_n^r(t),\quad t\in\mathbb{R}^+, \tag{8}$$

where u^r and f_n^r represent the normalized out-of-plane control force and disturbance force (their actual values should be multiplied by L_k) applied at the end of the rth string, respectively. r means the number of the exterior strings, and $r=13,14,\ldots,30$.

The initial conditions are

$$w^k(0,x)=w_0^k(x),\ w_t^k(0,x)=w_1^k(x),\quad x\in(0,1). \tag{9}$$

where $w_0^k(x)$ and $w_1^k(x)$ for the interior strings are equal to zero to avoid standing waves in the circuits.

Eqs. (3)–(9) compose an initial–boundary value problem, which describes the dynamics of the planar cable net structure with boundary control when it experiences disturbance forces at the boundary cables.

2.3. Wave-based boundary control strategy

In this paper, we adopt a boundary control method similar to the wave-absorbing method, which is one type of the wave-based vibration control methods, as the control strategy for the cable net structure. The idea of wave-absorbing control is to absorb the reflected waves at the boundaries of the exterior cables. If all the waves are absorbed, no vibration will be formed in the entire cable net structure.

First, we use a simple model of a single string to explain the mechanism of the wave-absorbing control. The normalized wave equation for this string is given as

$$w_{tt}(t,x)=c^2 w_{xx}(t,x),\ \text{in}\ \mathbb{R}^+\times(0,1). \tag{10}$$

Taking Laplace transforms of Eq. (10) with zero initial condition $w(0,x)=0$, the resulting boundary value problem is described by equation

$$s^2\hat{w}(s,x)=c^2\frac{\mathrm{d}^2\hat{w}(s,x)}{\mathrm{d}x^2}. \tag{11}$$

The general solution of Eq. (11) is

$$\hat{w}(s,x)=Ae^{xs/c}+Be^{-xs/c} \tag{12}$$

where $Ae^{xs/c}$ and $Be^{-xs/c}$ are considered as two waves traveling in the negative and positive directions along the string, respectively.

Then, applying Neumann boundary type control onto the end ($x=1$) of the string, whose form in the time domain is given as

$$Tw_x(t,1)=u(t), \tag{13}$$

where T is the normalized tension and $u(t)$ is the control law to be determined.

The wave-absorbing control, similar to D.L. Russell's work [28], takes the transverse velocity at the end of the string as the feedback signal of the control law, i.e.

$$u(t)=-Kw_t(t,1). \tag{14}$$

Combining Eqs. (13) and (14), we get the closed-loop boundary condition, which expressed in the complex frequency domain is

$$\frac{\mathrm{d}\hat{w}(s,1)}{\mathrm{d}x} = -\frac{s}{c}\hat{w}(s,1), \tag{15}$$

if we choose $K = T/c$.

Taking Eq. (12) to the closed-loop boundary condition Eq. (15), the solution under control is given as

$$\hat{w}(s,x) = Be^{-xs/c}. \tag{16}$$

This solution only contains one wave traveling in the positive direction, not satisfying the form of vibration. When the wave travels by the controlled point, the reflected wave (wave traveling in the negative direction) is canceled and the transmitted wave (wave traveling in the positive direction) is passed by. The waves seem to be absorbed at this point and the energy is also dissipated.

Now consider the cable net structure. The waves are transmitted from the external to the internal along the strings, and then continue to propagate from one string to the others according to certain laws. Similar to the simple single string with wave-absorbing control, the control strategy at every exterior node of the cable net structure is

$$u^r(t) = -K_r w_t^r(t,1), r = 13,\ldots,30, \tag{17}$$

where $K_r > 0$. The aim of this control strategy is to absorb or partially absorb the outgoing waves at the exterior nodes. Thus, the effect of disturbance will be gradually weakened whenever the wave generated by the disturbance passes through these exterior nodes.

Here the wave-based boundary control strategy is a collocated control method with velocity feedback. For physical implementation, the collocated control architecture can be attached near the support corners [16,29]. Ref. [14] pointed out that collocated actuating and sensing elements can be achieved by active cable structures [7] or by a tendon actuator collocated with a force sensor [30]. The method has been proposed to the vibration control of membrane structures [29] and axially moving strings [16]. It is noted that our wave-based boundary control with velocity feedback is exactly the same as a viscous damper tuned to impedance matching the characteristic impedance of the string attached at the end [31]. The collocated control method with velocity feedback can also be phrased in term of impedance matching, namely,

$$K_r = -u^r(t)/w_t^r(t,1) = T/c, r = 13,\ldots,30, \tag{18}$$

where K_r is the best impedance matching. However, the outgoing waves can also be absorbed by some other methods such as the non-collocated controller with displacement feedback [16], which is different from the velocity feedback with impedance matching.

3. Transfer function analysis of the controlled cable net

Unlike lumped-parameter systems, whose transfer functions are rational functions, the transfer functions of distributed-parameter systems are irrational ones. Ref. [32] illustrates the differences between the irrational transfer functions and the rational transfer functions and points out that boundary conditions have strong effects on the dynamics and the properties of the transfer function, such as the location of poles and zeros. In this section, we derive the transfer functions from the disturbances to the displacement of the cables in the cable net structure; and give the stability results of the structure under wave-based boundary controls by pole analysis.

When the normalized tensions T_k and linear densities ρ_k of the cables are different, the transfer functions are quite complicated, or even hard to be obtained. Here for simplicity of showing the explicit transfer functions and analyzing the distributions of their poles, we first consider T_k and ρ_k in each string to be the same, also resulting in the same wave velocity in each string. The same tension and wave velocity are denoted by T and c, respectively. Then, in Section 4, we will discuss the strings with different tensions, linear densities, and lengths by numerical method.

3.1. Disturbance applied at the exterior nodes

In this situation, $f_e^k(t,x) = 0$ and $f_n^r(t) \neq 0$. Taking Laplace transforms of Eqs. (3)–(8) and Eq. (17) with zero initial condition $w^k(\cdot,0) = 0$ and denoting the Laplace transforms of w^k and f_n^r by $\hat{w}^k$ and $\hat{f}_n^r$, respectively, the resulting equations are

$$c^2\frac{\mathrm{d}^2\hat{w}^k(s,x)}{\mathrm{d}x^2} - s^2\hat{w}^k(s,x) = 0, \quad x \in (0,1), \tag{19}$$

$$\hat{w}^i(s,0) = \hat{w}^j(s,0), \forall i,j \in I_{\mathbf{v}_1}, \tag{20}$$

$$\sum_{i\in I_{\mathbf{v}_1}}\frac{\mathrm{d}\hat{w}^i(s,0)}{\mathrm{d}x} = 0, \tag{21}$$

$$\hat{w}^{i_1}(s,1)=\hat{w}^{i_2}(s,1)=\hat{w}^{i_3}(s,0)=\hat{w}^{i_4}(s,0)=\hat{w}^{i_5}(s,0)=\hat{w}^{i_6}(s,0), \tag{22}$$

$$\frac{\mathrm{d}\hat{w}^{i_1}(s,1)}{\mathrm{d}x}+\frac{\mathrm{d}\hat{w}^{i_2}(s,1)}{\mathrm{d}x}-\frac{\mathrm{d}\hat{w}^{i_3}(s,0)}{\mathrm{d}x}-\frac{\mathrm{d}\hat{w}^{i_4}(s,0)}{\mathrm{d}x}-\frac{\mathrm{d}\hat{w}^{i_5}(s,0)}{\mathrm{d}x}-\frac{\mathrm{d}\hat{w}^{i_6}(s,0)}{\mathrm{d}x}=0, \tag{23}$$

$$T\frac{\mathrm{d}\hat{w}^{r}(s,1)}{\mathrm{d}x}=\hat{u}^{r}(s)+\hat{f}_n^{r}(s), \tag{24}$$

$$\hat{u}^{r}(s)=-K_r s\hat{w}^{r}(s,1), \tag{25}$$

where the values of k, i_1, i_2, i_3, i_4, i_5, i_6 and r are the same as aforementioned. The general solution of the ordinary differential equation (19) is

$$\hat{w}^{k}(s,x)=A_k e^{xs/c}+B_k e^{-xs/c}, \tag{26}$$

where A_k and B_k are the coefficients determined by the boundary conditions (20)–(25). Combining Eqs. (20)–(26), by some calculations, we obtain A_k and B_k, which are expressions of $\hat{f}_n^r$. Then substituting A_k and B_k into Eq. (26), the response of the kth string will be obtained regarding $\hat{f}_n^r$, i.e.

$$\hat{w}^{k}(s,x)=\sum_{r=13}^{30}G_n^{k,r}(s,x)\hat{f}_n^{r}(s), \tag{27}$$

where $G_n^{k,r}(s,x)$ represents the transfer function from the force applied at the outer end of the rth string to the displacement at $x(0\le x\le 1)$ of the kth string.

Due to linearity, we only consider the disturbance force applied at the outer end of the 16th string, i.e. $f_n^r(t)=0, r=13,\ldots,15,17,\ldots,30$, and $f_n^{16}(t)=f(t)$. We choose the 2nd and the 16th string to explicitly show their transfer functions, while the rest are in the similar forms. When $K_r=T/c$, the transfer functions from f to the displacement of the mentioned strings at x are

$$\begin{aligned}G_n^{2,16}(s,x)=&\frac{c(81e^{-\frac{(2-x)s}{c}}+81e^{-\frac{(3-x)s}{c}}+63e^{-\frac{(4-x)s}{c}}+21e^{-\frac{(5-x)s}{c}}-2e^{-\frac{(6-x)s}{c}})}{6(3+e^{-\frac{s}{c}})(3-e^{-\frac{s}{c}})(3+2e^{-\frac{s}{c}})(3+e^{-\frac{s}{c}}+2e^{-\frac{2s}{c}})Ts}\\&-\frac{c(54e^{-\frac{(2+x)s}{c}}+36e^{-\frac{(3+x)s}{c}}+48e^{-\frac{(4+x)s}{c}}+26e^{-\frac{(5+x)s}{c}})}{6(3+e^{-\frac{s}{c}})(3-e^{-\frac{s}{c}})(3+2e^{-\frac{s}{c}})(3+e^{-\frac{s}{c}}+2e^{-\frac{2s}{c}})Ts},\end{aligned} \tag{28}$$

$$\begin{aligned}G_n^{16,16}(s,x)=&\frac{c(243e^{-\frac{(1-x)s}{c}}+243e^{-\frac{(2-x)s}{c}}+189e^{-\frac{(3-x)s}{c}}+81e^{-\frac{(4-x)s}{c}}-24e^{-\frac{(5-x)s}{c}}-12e^{-\frac{(6-x)s}{c}})}{6(3+e^{-\frac{s}{c}})(3-e^{-\frac{s}{c}})(3+2e^{-\frac{s}{c}})(3+e^{-\frac{s}{c}}+2e^{-\frac{2s}{c}})Ts}\\&-\frac{c(162e^{-\frac{(1+x)s}{c}}+162e^{-\frac{(2+x)s}{c}}+180e^{-\frac{(3+x)s}{c}}+96e^{-\frac{(4+x)s}{c}}+26e^{-\frac{(5+x)s}{c}}+14e^{-\frac{(6+x)s}{c}})}{6(3+e^{-\frac{s}{c}})(3-e^{-\frac{s}{c}})(3+2e^{-\frac{s}{c}})(3+e^{-\frac{s}{c}}+2e^{-\frac{2s}{c}})Ts}.\end{aligned} \tag{29}$$

The poles of these transfer functions, by some mathematical calculations, are composed by

$$0,\ c(\ln\frac{1}{3}+\mathrm{i}N\pi),\ c(\ln\frac{2}{3}+\mathrm{i}2N\pi),\ c(\ln\frac{2\sqrt{6}}{6}+\mathrm{i}(\pm\arctan(\sqrt{23})+2N\pi)),\ N=0,\pm1,\pm2,\ldots \tag{30}$$

All those transfer functions have a zero pole and infinitely many complex poles with a negative real part, which represent the rigid mode and the flexible modes with damping, respectively. Since all the flexible modes have damping, the energy of the strings will finally decay to zero and the induced vibration can be resisted.

Now consider a situation where only one external cable with fixed outer end experiences no disturbance (Take the 15th string for example), while the other external cables may still experience disturbance from the exterior nodes. We further check the stability of the net structure under controls. The boundary conditions for the external cables (Eq. (24)) becomes

$$\hat{w}^{15}(s,1)=0,\quad T\frac{\mathrm{d}\hat{w}^{r}(s,1)}{\mathrm{d}x}=-K_r s\hat{w}^{r}(s,1)+\hat{f}_n^{r}(s),\ r\neq 15. \tag{31}$$

Substituting Eqs. (20)–(23) and Eq. (31) into Eq. (26), the solutions of the responses in the complex frequency domain can be obtained. When $K_r=T/c$, the transfer function from the force disturbance applied at the outer end of the 16th string to the displacement of the 2nd string is expressed as follows, while the others are of the familiar form.

$$\begin{aligned}G_{n1}^{2,16}(s,x)=&\frac{c(81e^{-\frac{(2-x)s}{c}}-18e^{-\frac{(4-x)s}{c}}-42e^{-\frac{(5-x)s}{c}}-23e^{-\frac{(6-x)s}{c}}+2e^{-\frac{(7-x)s}{c}})}{2(243+27e^{-\frac{2s}{c}}-108e^{-\frac{3s}{c}}-96e^{-\frac{4s}{c}}-12e^{-\frac{5s}{c}}-14e^{-\frac{6s}{c}})Ts}\\&-\frac{c(54e^{-\frac{(2+x)s}{c}}-18e^{-\frac{(3+x)s}{c}}+12e^{-\frac{(4+x)s}{c}}-22e^{-\frac{(5+x)s}{c}}-26e^{-\frac{(6+x)s}{c}})}{2(243+27e^{-\frac{2s}{c}}-108e^{-\frac{3s}{c}}-96e^{-\frac{4s}{c}}-12e^{-\frac{5s}{c}}-14e^{-\frac{6s}{c}})Ts}.\end{aligned} \tag{32}$$

The characteristic polynomial is more sophisticated than that of $G_n^{2,16}(s,x)$. It is obvious to find that $s=0$ is a pole of the transfer function, while the other poles are determined by the function of the following form

$$p(s)=a_N+a_{N-1}e^{-s/c}+\cdots+a_1e^{-(N-1)s/c}+a_0e^{-Ns/c},\quad a_N\neq 0 \tag{33}$$

It is important to know whether each of the solutions of the equation $p(s)=0$ has a negative real part. Let $z=e^{s/c}$, since $a_N\neq 0, z\neq 0$, then $p(s)=0$ is equal to $p(z)=0$, where $p(z)$ is of the following form

$$p(z)=a_0+a_1z+a_2z^2+\cdots+a_{N-1}z^{N-1}+a_Nz^N \tag{34}$$

From Jury stability criterion [33], it is easy to check whether all the solutions associated with $p(z)=0$ are located inside the unit circle or not, i.e. whether $|z|<1$ or not, by the coefficients a_n in Eq. (34). If $|z|<1$, then s, i.e the poles of the transfer function, lie in the left half s-plane. By this method, we find that $G_{n1}^{2,16}(s,x)$ has a zero pole and infinitely many complex poles with negative real parts. So the vibration can also be resisted when all the outer ends of the external cables, which experience disturbances, are applied with our boundary control strategy.

When the outer end of an external cable without control experiences disturbances, the transfer function is not available, since the boundary condition at this end changes from a forced boundary condition to a fixed boundary condition. In this situation, this stability analysis is carried out by using a numerical method (shown in Section 4). It is found that the induced waves cannot be absolutely absorbed and result in the vibration in the cable net.

3.2. Disturbance applied at the exterior edges

In this situation, $f_n^r=0$ and $f_e^k(t,x)\neq 0$. Due to linearity, we only consider the disturbance force applied on the 16th string. While the other strings experience no disturbances. Thus, $f_e^k(t,x)=0, k\neq 16$. Let $f_e^{16}(t,x)=\delta(x-x_0)f(t)$, where $0<x_0<1$ and $\delta(\cdot)$ is a Dirac delta function. Denoting the Laplace transform of f by $\hat{f}$, then Eq. (19) becomes

$$c^2\frac{\mathrm{d}^2\hat{w}^k(s,x)}{\mathrm{d}x^2}-s^2\hat{w}^k(s,x)=0,\ x\in(0,1), k\neq 16, \tag{35}$$

$$c^2\frac{\mathrm{d}^2\hat{w}^{16}(s,x)}{\mathrm{d}x^2}-s^2\hat{w}^{16}(s,x)=\delta(x-x_0)\hat{f}(s)\,, x\in(0,1). \tag{36}$$

Combining Eqs. (20)–(25), Eqs. (35)–(36) with $f_n^r=0$, in a similar way, we can obtain the transfer functions from the disturbance to the displacement of the strings. We choose the 2nd and the 16th string to explicitly show their transfer functions. When $K_r=T/c$, these transfer functions are expressed as

$$\begin{aligned}G_e^{2,16}(s,x)=&\frac{ce^{-\frac{(x_0-1)s}{c}}(81e^{-\frac{(2-x)s}{c}}+81e^{-\frac{(3-x)s}{c}}+63e^{-\frac{(4-x)s}{c}}+21e^{-\frac{(5-x)s}{c}}-2e^{-\frac{(6-x)s}{c}})}{6(3+e^{-\frac{s}{c}})(3-e^{-\frac{s}{c}})(3+2e^{-\frac{s}{c}})(3+e^{-\frac{s}{c}}+2e^{-\frac{2s}{c}})Ts}\\&-\frac{ce^{-\frac{(x_0-1)s}{c}}(54e^{-\frac{(2+x)s}{c}}+36e^{-\frac{(3+x)s}{c}}+48e^{-\frac{(4+x)s}{c}}+26e^{-\frac{(5+x)s}{c}})}{6(3+e^{-\frac{s}{c}})(3-e^{-\frac{s}{c}})(3+2e^{-\frac{s}{c}})(3+e^{-\frac{s}{c}}+2e^{-\frac{2s}{c}})Ts},\end{aligned} \tag{37}$$

$$\begin{aligned}G_e^{16,16}(s,x)=&\frac{ce^{-\frac{x_0s}{c}}(243e^{\frac{xs}{c}}+243e^{-\frac{(1-x)s}{c}}+189e^{-\frac{(2-x)s}{c}}+81e^{-\frac{(3-x)s}{c}}-24e^{-\frac{(4-x)s}{c}}-12e^{-\frac{(5-x)s}{c}})}{6(3+e^{-\frac{s}{c}})(3-e^{-\frac{s}{c}})(3+2e^{-\frac{s}{c}})(3+e^{-\frac{s}{c}}+2e^{-\frac{2s}{c}})Ts}\\&-\frac{ce^{-\frac{x_0s}{c}}(162e^{-\frac{xs}{c}}+162e^{-\frac{(1+x)s}{c}}+180e^{-\frac{(2+x)s}{c}}+96e^{-\frac{(3+x)s}{c}}+26e^{-\frac{(4+x)s}{c}}+14e^{-\frac{(5+x)s}{c}})}{6(3+e^{-\frac{s}{c}})(3-e^{-\frac{s}{c}})(3+2e^{-\frac{s}{c}})(3+e^{-\frac{s}{c}}+2e^{-\frac{2s}{c}})Ts},\\&0\leq x<x_0,\end{aligned} \tag{38}$$

$$\begin{aligned}G_e^{16,16}(s,x)=&\frac{c(243e^{-\frac{xs}{c}}+243e^{-\frac{(1+x)s}{c}}+189e^{-\frac{(2+x)s}{c}}+81e^{-\frac{(3+x)s}{c}}-24e^{-\frac{(4+x)s}{c}}-12e^{-\frac{(5+x)s}{c}})}{6(3+e^{-\frac{s}{c}})(3-e^{-\frac{s}{c}})(3+2e^{-\frac{s}{c}})(3+e^{-\frac{s}{c}}+2e^{-\frac{2s}{c}})Ts}\\&-\frac{ce^{-\frac{(x+2x_0)s}{c}}(162+162e^{-\frac{s}{c}}+180e^{-\frac{2s}{c}}+96e^{-\frac{3s}{c}}+26e^{-\frac{4s}{c}}+14e^{-\frac{5s}{c}})}{6(3+e^{-\frac{s}{c}})(3-e^{-\frac{s}{c}})(3+2e^{-\frac{s}{c}})(3+e^{-\frac{s}{c}}+2e^{-\frac{2s}{c}})Ts},\ x_0\leq x\leq 1.\end{aligned} \tag{39}$$

Note that the only difference between $G_e^{2,16}(s,x)$ and $G_n^{2,16}(s,x)$ is the item $e^{-(x_0-1)s/c}$, which represents a time delay, i.e. the response of $G_e^{2,16}(s,x)$ is earlier than that of $G_n^{2,16}(s,x)$ and the time difference is $t=(1-x_0)/c$. The poles of $G_e^{2,16}(s,x)$ and $G_e^{16,16}(s,x)$ are the same as those of $G_n^{2,16}(s,x)$ and $G_n^{16,16}(s,x)$. All the flexible modes have damping, so the induced waves can be absorbed and vibration will not form in the cable net.

Now consider the wave-based boundary controllers are applied at the outer ends of all the external cables except the end of one string (the 15th or 16th string), while the disturbance is applied at x_0 of the 16th string. The boundary conditions are

similar to Eq. (31). When the only one uncontrolled string is the 15th string, the transfer function from the force disturbance to the displacement of the 2nd string is expressed as follows,

$$G_{e1}^{2,16}(s,x)=\frac{ce^{-\frac{(x_0-1)s}{c}}(81e^{-\frac{(2-x)s}{c}}-18e^{-\frac{(4-x)s}{c}}-42e^{-\frac{(5-x)s}{c}}-23e^{-\frac{(6-x)s}{c}}+2e^{-\frac{(7-x)s}{c}})}{2(243+27e^{-\frac{2s}{c}}-108e^{-\frac{3s}{c}}-96e^{-\frac{4s}{c}}-12e^{-\frac{5s}{c}}-14e^{-\frac{6s}{c}})Ts}$$
$$-\frac{ce^{-\frac{(x_0-1)s}{c}}(54e^{-\frac{(2+x)s}{c}}+18e^{-\frac{(3+x)s}{c}}-12e^{-\frac{(4+x)s}{c}}+22e^{-\frac{(5+x)s}{c}}+26e^{-\frac{(6+x)s}{c}})}{2(243+27e^{-\frac{2s}{c}}-108e^{-\frac{3s}{c}}-96e^{-\frac{4s}{c}}-12e^{-\frac{5s}{c}}-14e^{-\frac{6s}{c}})Ts}. \tag{40}$$

When the 16th string is the only one uncontrolled string, the corresponding transfer function is

$$G_{e2}^{2,16}(s,x)=\frac{c(81e^{-\frac{(1-\eta)s}{c}}+81e^{-\frac{(2-\eta)s}{c}}+63e^{-\frac{(3-\eta)s}{c}}+81e^{-\frac{(4-\eta)s}{c}}-2e^{-\frac{(5-\eta)s}{c}})}{2(1+e^{-\frac{s}{c}})(243+27e^{-\frac{2s}{c}}-108e^{-\frac{3s}{c}}-96e^{-\frac{4s}{c}}-12e^{-\frac{5s}{c}}-14e^{-\frac{6s}{c}})Ts}$$
$$+\frac{c(54e^{-\frac{(3+\eta)s}{c}}+36e^{-\frac{(4+\eta)s}{c}}+48e^{-\frac{(5+\eta)s}{c}}+26e^{-\frac{(6+\eta)s}{c}})}{2(1+e^{-\frac{s}{c}})(243+27e^{-\frac{2s}{c}}-108e^{-\frac{3s}{c}}-96e^{-\frac{4s}{c}}-12e^{-\frac{5s}{c}}-14e^{-\frac{6s}{c}})Ts}$$
$$-\frac{c(81e^{-\frac{(3-\gamma)s}{c}}+81e^{-\frac{(4-\gamma)s}{c}}+63e^{-\frac{(5-\gamma)s}{c}}+21e^{-\frac{(6-\gamma)s}{c}}-2e^{-\frac{(7-\gamma)s}{c}})}{2(1+e^{-\frac{s}{c}})(243+27e^{-\frac{2s}{c}}-108e^{-\frac{3s}{c}}-96e^{-\frac{4s}{c}}-12e^{-\frac{5s}{c}}-14e^{-\frac{6s}{c}})Ts}$$
$$-\frac{c(54e^{-\frac{(1+\gamma)s}{c}}+36e^{-\frac{(2+\gamma)s}{c}}+48e^{-\frac{(3+\gamma)s}{c}}+26e^{-\frac{(4+\gamma)s}{c}})}{2(1+e^{-\frac{s}{c}})(243+27e^{-\frac{2s}{c}}-108e^{-\frac{3s}{c}}-96e^{-\frac{4s}{c}}-12e^{-\frac{5s}{c}}-14e^{-\frac{6s}{c}})Ts}, \tag{41}$$

where $\gamma=x+x_0$ and $\eta=x-x_0$.

By Jury stability criterion we find that both $G_{e1}^{2,16}(s,x)$ and $G_{e2}^{2,16}(s,x)$ have infinitely many complex poles with negative real parts. However, in the denominator of $G_{e2}^{2,16}(s,x)$ there is an item $1+e^{-s/c}$, which relates to infinitely many pure imaginary poles: $\mathrm{i}c(2N+1)\pi$, $N=0,\pm1,\pm2,\ldots$. In other words, all the flexible modes of $G_{e1}^{2,16}(s,x)$ have damping, while the damping does not exist for infinitely many flexible modes of $G_{e2}^{2,16}(s,x)$. So when the disturbance is applied at x_0 of the 16th string, the induced waves can be absolutely absorbed or just be partially absorbed if the only one uncontrolled string is the 15th string or the 16th string, respectively. Fewer controllers are possible to resist the formation of vibration induced by the disturbance applied at the exterior edges, but the locations of the missing controllers should be carefully chosen. This result will also be verified by the numerical method in Section 4.

4. Numerical simulations

In order to verify the effectiveness of the wave-based boundary control strategy, the Lax–Friedrichs scheme is employed to analyze the out-of-plane vibration of the planar cable net structures. The numerical scheme for the cable net structure is firstly presented, where the normalized tension and linear densities are the same in each string (so that the normalized wave velocities are also the same). The structural dynamic responses, with no control and several different wave-based boundary control strategies, are then compared and analyzed. Case studies are also conducted when the physical and geometrical parameters in each string are different.

4.1. Lax–Friedrichs scheme for the planar cable net structure

The Lax–Friedrichs scheme, which is an FTCS (forward in time, centered in space) method for the numerical solution of hyperbolic partial differential equations, was first proposed in Ref. [34]. It is explicit and first order accurate in time and first order accurate in space, provided the initial values and boundary values are sufficiently-smooth functions. Under these conditions, the method is stable if and only if the Courant number is less or equal to 1. In the case that the initial or boundary values have discontinuities, the scheme displays strong dissipation and dispersion which must be noted.

Applying this scheme, the iterative equation for $\dot{f}=cg'$ (superimposed dot and prime respectively mean time and space derivative) is represented as

$$f_p^{q+1}=\frac{1}{2}(f_{p+1}^q+f_{p-1}^q)+\frac{\alpha}{2}(g_{p+1}^q-g_{p-1}^q), \tag{42}$$

where p and q represent the steps of the discretized space and time on a grid, respectively, and $\alpha=c\Delta t/\Delta x$ is the Courant number, which should not exceed 1 for numerical stability.

As for the cable net structure, we first consider the disturbance applied at the exterior nodes, i.e. $f_e^k(t,x)=0$. Let $u_k=cw_x^k$, $v_k=w_t^k$, then the homogeneous wave equations of Eq. (3) are transformed to first order equations

$$\dot{u}_k=cv_k', \quad \dot{v}_k=cu_k'. \tag{43}$$

The domain $[0, T] \times [0, 1]$ is discretized into a grid $x_p = p \cdot \Delta x, p = 0, \ldots, m, t_q = q \cdot \Delta t, q = 0, \ldots, n$ for each string, where $\Delta x = 1/m$, $\Delta t = \alpha \cdot \Delta x/c$. Then $u_k(t_q, x_p)$ is represented by $u^q_{k,p}$.

When the initial conditions are given, by applying the Lax–Friedrichs scheme Eq. (42) to Eq. (43), we can get the system response by iterations

$$\begin{cases} u^{q+1}_{k,p} = \frac{1}{2}(u^q_{k,p+1} + u^q_{k,p-1}) + \frac{\alpha}{2}(v^q_{k,p+1} - v^q_{k,p-1}) \\ v^{q+1}_{k,p} = \frac{1}{2}(v^q_{k,p+1} + v^q_{k,p-1}) + \frac{\alpha}{2}(u^q_{k,p+1} - u^q_{k,p-1}). \end{cases} \tag{44}$$

Note that some auxiliary points $(u^q_{k,-1}, v^q_{k,-1}, u^q_{k,m+1}, v^q_{k,m+1})$, which are called ghost points (c.f. [35], section 1.4), are needed to calculate the values of points at the boundaries ($p = 0$ and $p = m$). For the interior nodes and the exterior nodes with different boundary conditions, the calculation on the values of the ghost points can be seen in Appendix A. Once $v^q_{k,p}$ is known, $w^k(t_q, x_p)$ can be calculated by

$$w^{q+1}_{k,p} = w^q_{k,p} + v^q_{k,p}\Delta t. \tag{45}$$

When the disturbance is applied at a point of an exterior edge, the numerical scheme is similar to the procedure presented above, except that the exterior edge is divided into two segments and another auxiliary node is presented. The above scheme is implemented in Matlab for numerical analysis of the cable net structure.

4.2. Simulation results

We first study the wave-based boundary control of the cable net, where each string has the same tension T, the same linear density ρ, and the same length L. They are all set to be 1. The parameters of the numerical scheme are as follows: the time step $\Delta t = 0.01s$, the Courant number $\alpha = 1$ [36], and the space step $\Delta x = 0.01$. Since Eqs. (8) and (17) represent a transparent boundary condition when $K_r = T/c$, i.e, the solution of the boundary value problem is exactly the solution of the initial problem, which means this boundary condition is numerically useless [37]. Thus, we set $K_r = 0.99T/c$, to appropriate the absorbing boundary condition. The wave-absorbing control is achieved by the wave-based boundary control with this feedback gain K_r in the numerical method.

Six different cases are studied: no control; wave-absorbing controls applied at all the exterior nodes (control strategy 1, Fig. 2(a)); wave-based boundary controls applied at all the exterior nodes with feedback gains changed to be $K_r = 0.5T/c$ (control strategy 2, Fig. 2(a)); some exterior nodes ($\mathbf{v}_8$-$\mathbf{v}_{16}$) applied with wave-absorbing controls (control strategy 3, Fig. 2(b)); wave-absorbing controls applied at all the exterior nodes except the exterior node $\mathbf{v}_8$, which experiences a force disturbance (control strategy 4, Fig. 2(c)). wave-absorbing controls applied at all the exterior nodes except the exterior node $\mathbf{v}_{15}$ in the string, which experiences a force disturbance (control strategy 5, Fig. 2(d)).

Two force disturbances are applied to the cable net simultaneously. One is applied at $x = 0.4$ of the 23rd string and the other is applied at the outer end of the 16th string, they are denoted by f_1 and f_2, respectively (see Fig. 2). The normalized values of the two forces are $f(t) = 10\sin(10\pi t)\,(0 < t <= 0.2s)$ and $f(t) = 0(t > 0.2s)$. All the strings have no initial displacement and velocities. Thus, all the initial and boundary values are smooth functions in the time intervals $[0, 0.2]$ and $(0.2, \infty]$, separately. Since the Courant number is 1, the numerical method is stable and the numerical solutions approximate the real system quite well. At $t = 0.2s$, the force f_2 applied at the outer end of the 16th string is removed, resulting in $f(t)$ equal to zero. The boundary condition of the exterior node without control is therefore continuous and both the dissipation and dispersion can be prevented.

Considering the cases where the structure is uncontrolled and with control strategies 1, 3 and 5, the dynamic responses of the cable net structure at time $t = 0.12$ s, $t = 0.24$ s, $t = 0.80$ s, $t = 10.02$ s, and $t = 20.02$ s are shown in Fig. 3. The Figure shows that control strategies 1 and 3 can resist the formation of vibration induced by disturbances from the external boundary cables, while control strategy 5 cannot. This can be explained as follows.

Boundary control is applied at all the exterior nodes of the structure, which can affect all the flexible modes, thus control strategies 1 and 3 are able to affect the flexible modes activated by the force disturbance f_2 applied at the exterior node. On the other hand, we can see from Fig. 3 that f_2 generates an one-way wave, while f_1 generates two waves traveling in the opposite directions ($t = 0.24$ s). When node $\mathbf{v}_{15}$ is under wave-absorbing control, the outgoing wave will be absorbed. So only a one-way wave will travel into the internal of the cable net (Fig. 3(b) and (c), $t = 0.80$ s). The effect of f_1 is equivalent to that of f_2 when node $\mathbf{v}_{15}$ is under wave-absorbing control. In other words, control strategies 1 and 3 are also able to affect the flexible modes activated by f_1 when the boundary conditions of the external cables are unchanged.

However, the effect of f_1 cannot be equivalent to that of f_2 when control strategy 5 is adopted (In Fig. 3(d), $t = 0.8$ s), since the outgoing wave generated by f_1 cannot be absorbed by this control strategy. As a consequence, control strategy 5 cannot resist the formation of the vibration induced by the disturbances from the exterior cables.

When the feedback gain of the wave-based boundary control at node $\mathbf{v}_{15}$ is not equal to T/c, the outgoing wave is partially absorbed and the rest is reflected, without changing its sign. The effect of f_1 is also equivalent to generate two one-way waves at the exterior nodes, which travels into the internal of the cable net at different time. Thus, control strategy 2 is also able to resist the formation of the vibration, which is in consistent with the result obtained by transfer function analysis.

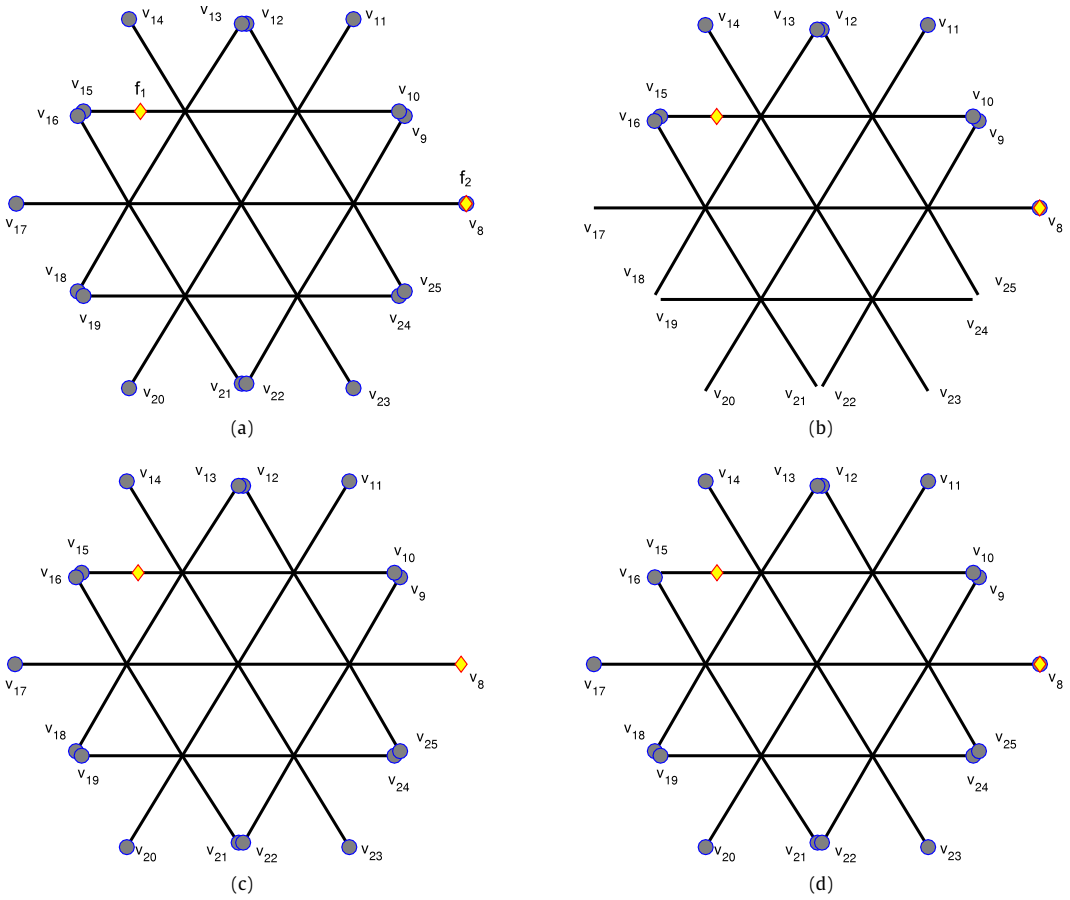

Fig. 2. The locations of the wave-based boundary controllers and the force disturbances: (a) control strategies 1 and 2; (b) control strategy 3; (c) control strategy 4; and (d) control strategy 5. The circles and diamonds represent the locations of the controls and the force disturbances, respectively.

The total energy of the cable net structure for the six cases is numerically computed, by applying the trapezoidal rule (see Appendix B). As shown in Fig. 4, the total energy increases at the beginning, due to the work done by the disturbance forces. Then the total energy becomes conservative when the net is uncontrolled, or decreases when the net is applied with wave-based boundary controllers. In comparison, only control strategies 1, 2, and 3 steer the total energy to zero. The result indicates that the cable net structure can resist the formation of vibration under these control strategies when the disturbances are applied at the exterior strings, which is consistent with the results obtained by pole analysis of the transfer functions in Section 3. The energy of the cable net with control strategy 2 decays slower than that with control strategy 1, which reveals that control strategy 1 is more efficient than control strategy 2, i.e. wave-absorbing controllers are more efficient than wave-based boundary controllers with feedback gains equal to $0.5T/c$. The energy of the cable net with control strategy 3 finally decreases to zero. This result shows that it is possible to reduce the number of the wave-based boundary controllers. However, the locations of the missing controllers must be carefully determined, otherwise, vibration may form in the cable net (control strategies 4 and 5).

The energy in the 6th, the 16th, and the 23rd strings for the first 4 cases are shown in Figs. 5–7. For a specific string, waves are traveling into and out of the string from time to time. The sudden incoming or outgoing of the waves causes the fluctuations of the energy of the strings, as shown in Figs. 5–7 (especially in the no control case). By using control strategies 1, 2, and 3, the energy of the three strings in the cable net structure all decreases to zero. This means that the cable net finally comes to rest in these three cases, while the non- dissipative energy causes the formation of vibration in the cable net structure under no control.

In order to check the effectiveness of the wave-based boundary control strategies in the case of cables with different physical and geometrical properties, we set the tension T_k, the linear densities ρ_k of each string with the values listed in Table 1, while the lengths of each string are 1.

The parameters listed in Table 1 represent that the cables in the same line (see Fig. 1) have the same tension and the same linear densities. This assures that the wave velocities in some of the strings are different. Note that the normalized and the

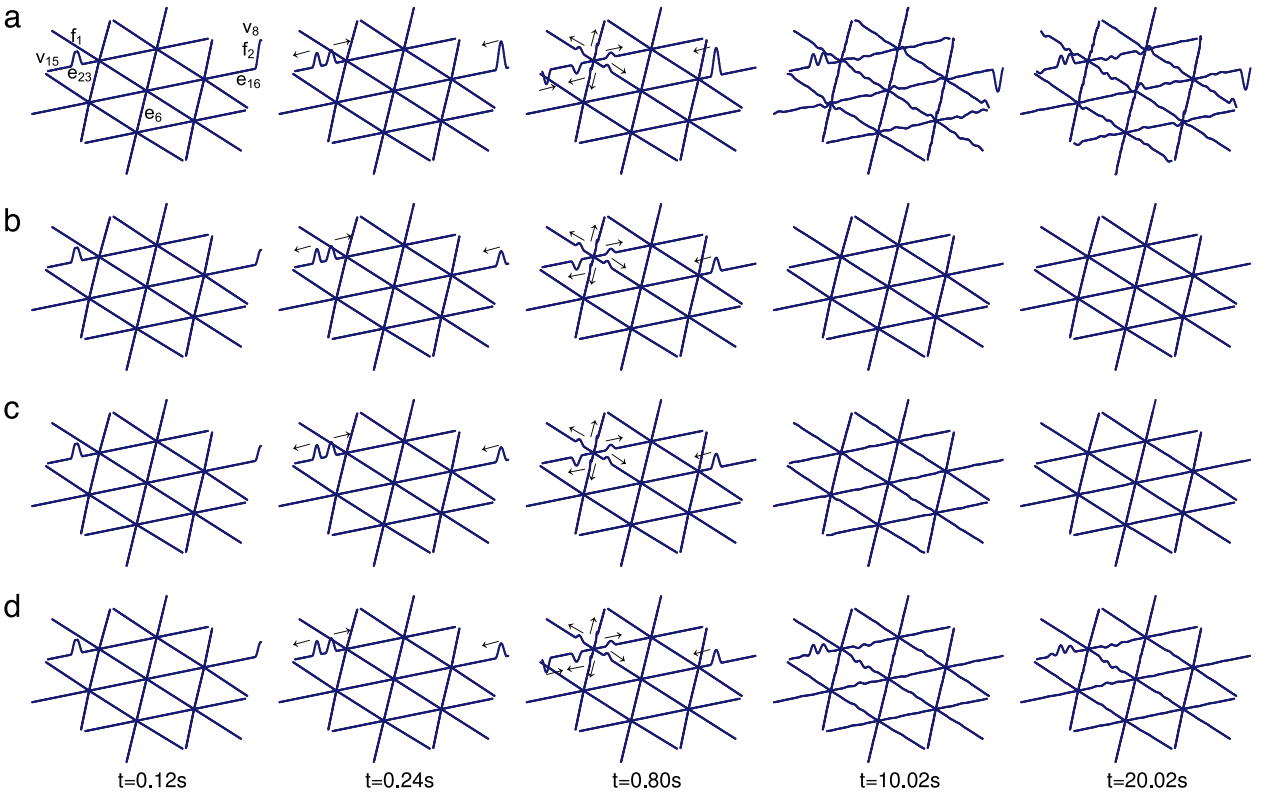

Fig. 3. Comparison of the out-of-plane displacement of the entire cable net structure at different time for the three cases: (a) no control; (b) control strategy 1; (c) control strategy 3; and (d) control strategy 5, where the parameters in each string are the same.

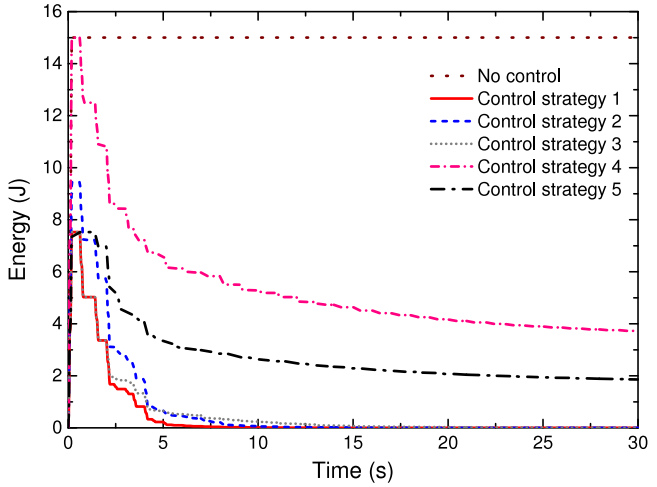

Fig. 4. Comparison of the total energy in the cable net structure with time for the six cases, where the parameters in each string are the same.

non-normalized parameters T_k, ρ_k, and c_k are the same in this situation. The data in the table retains two decimal places, but some c_k are actually irrational numbers.

We take the same six different cases as aforementioned, i.e. the cable net with no control, with control strategies 1, 2, 3, 4, and 5, with the same force disturbances and the same initial conditions as before. The simulation scheme is similar as illustrated in Section 4.1, however, there are some differences. Since the wave velocities of each string are not the same, the space steps for the strings are different according to $\Delta x_k = c_k \Delta t$. Besides, the calculation of the ghost points values is more sophisticated. In the following simulations, we set $\Delta t = 0.001s$.

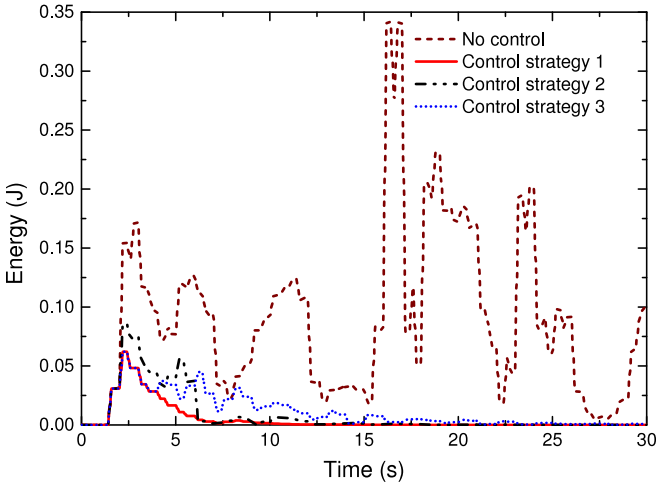

Fig. 5. Comparison of the energy in the 6th string of the cable net structure with time for the first 4 cases, where the parameters in each string are the same.

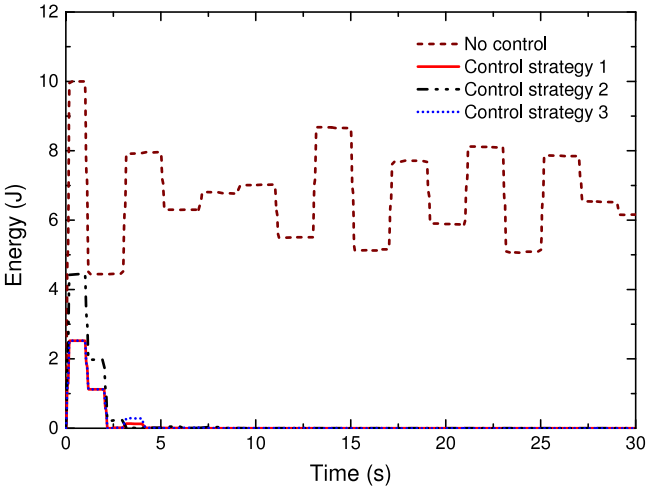

Fig. 6. Comparison of the energy in the 16th string of the cable net structure with time for the first 4 cases, where the parameters in each string are the same.

Table 1
Parameters of the strings in the cable net structure.

String no.	T_k (N)	ρ_k (kg/m)	c_k (m/s)	String no.	T_k (N)	ρ_k (kg/m)	c_k (m/s)	String no.	T_k (N)	ρ_k (kg/m)	c_k (m/s)
1	1.00	1.00	1.00	11	1.20	0.80	1.22	21	1.80	0.20	3.00
2	0.40	1.60	0.50	12	0.20	1.80	0.33	22	1.00	1.00	1.00
3	1.60	0.40	2.00	13	1.00	1.00	1.00	23	0.60	1.40	0.65
4	1.00	1.00	1.00	14	0.20	1.80	0.33	24	1.20	0.80	1.22
5	0.40	1.60	0.50	15	0.80	1.20	0.82	25	0.40	1.60	0.50
6	1.60	0.40	2.00	16	0.40	1.60	0.50	26	1.80	0.20	3.00
7	1.40	0.60	1.53	17	1.40	0.60	1.53	27	0.20	1.80	0.33
8	0.80	1.20	0.82	18	0.60	1.40	0.65	28	1.60	0.40	2.00
9	0.60	1.40	0.65	19	1.60	0.40	2.00	29	1.20	0.80	1.22
10	1.80	0.20	3.00	20	0.80	1.20	0.82	30	1.40	0.60	1.53

The total energy of the cable net structure for the six cases is shown in Fig. 8. It can be seen that the results are similar to Fig. 4 except that the control efficiency of control strategy 5 is improved. The reason is as follows. According to Refs. [38,39], the irrationality of c_i/c_j, where i and j are the indices of the strings in the circuit, can assure the waves not to be trapped in that circuit while traveling. Due to the change of c_i/c_j, the waves escape from the circuits more easily.

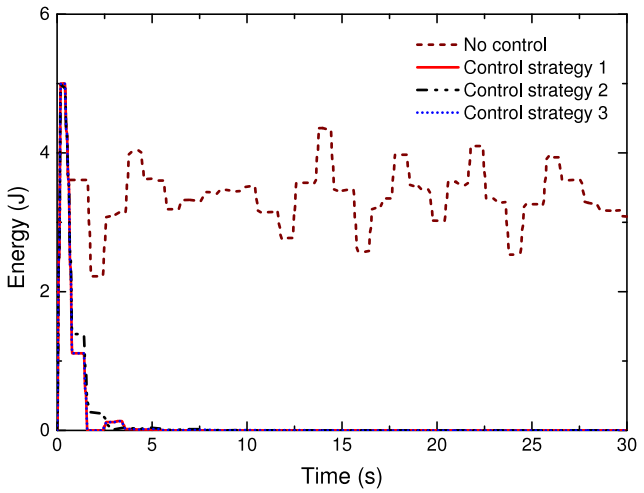

Fig. 7. Comparison of the energy in the 23rd string of the cable net structure with time for the first 4 cases, where the parameters in each string are the same.

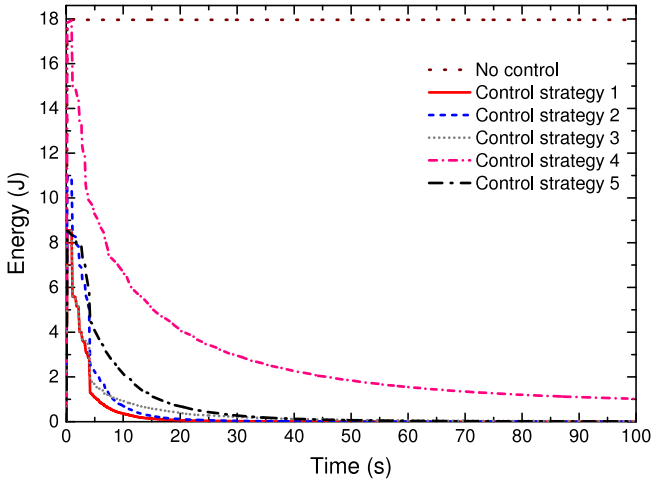

Fig. 8. Comparison of the total energy in the cable net structure with time for the six cases, where the parameters in some strings are different.

The energy in the 6th, 16th, and 23rd strings for the first 4 cases are shown in Figs. 9–11. Again, the results are similar to Figs. 5–7, showing that control strategies 1, 2, and 3 are effective even if the cables are with different physical and geometrical properties.

For vibrations induced by disturbances from the internal strings (strings in a circuit), the effectiveness of the wave-based boundary control strategy is determined by the physical and geometrical properties of the cables, i.e T_k, ρ_k, and L_k. Once the waves escape from the circuits while traveling, they would be absorbed by the wave-based boundary controllers, i.e., control strategies 1 and 2 are still effective; otherwise, the control strategies are ineffective. However, we can add a few more controllers from the internal nodes to absolutely control the vibrations in this case, which need study further.

5. Conclusion

This paper studies the vibration control of large cable net structures and the effectiveness of the wave-based boundary control strategies are investigated. For disturbance coming from the exterior boundary of the structure, the stability of the structure with our proposed control strategy is proved by using pole analysis of the transfer function and the numerical dynamic responses of the structure are achieved by using Lax–Friedrichs scheme. The results show that by imposing wave-based boundary controls at all the boundary nodes, the disturbances coming from the external can be absolutely absorbed. As a result, the structural vibration can be controlled efficiently. Comparing with the traditional modal control, the wave-based boundary control strategy avoids modal truncation and spillover effect, providing new avenues for vibration control on large cable net structures in many engineering fields.

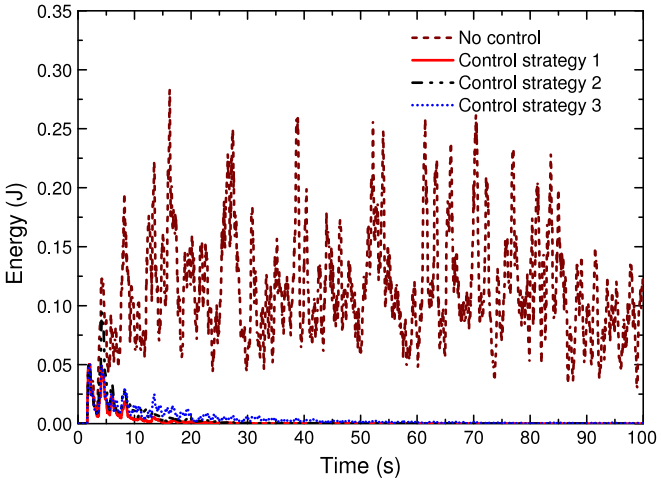

Fig. 9. Comparison of the energy in the 6th string of the cable net structure with time for the first 4 cases, where the parameters in some strings are different.

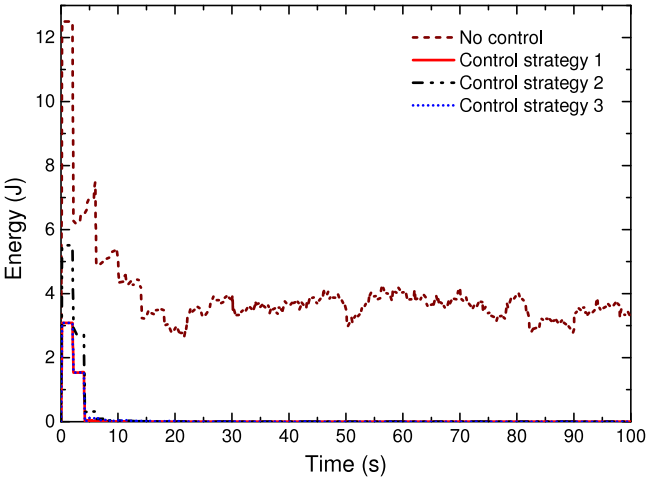

Fig. 10. Comparison of the energy in the 16th string of the cable net structure with time for the first 4 cases, where the parameters in some strings are different.

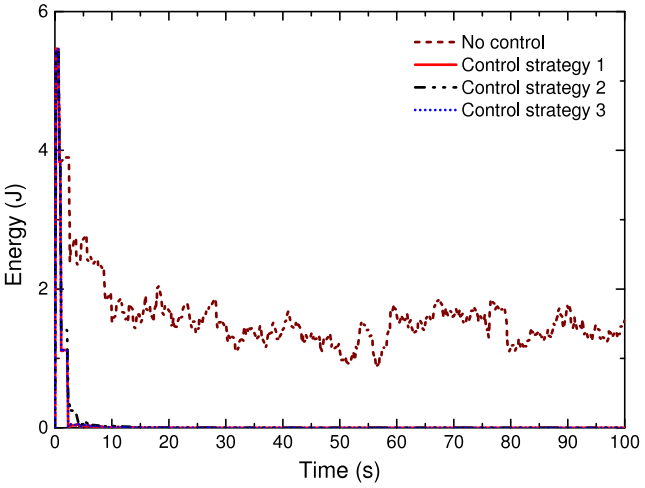

Fig. 11. Comparison of the energy in the 23rd string of the cable net structure with time for the first 4 cases, where the parameters in some strings are different.

Acknowledgment

This work was sponsored by the National Natural Science Foundation of China (Grant No. 11290153).

Appendix A. Calculation of the ghost points values

The values of the ghost points around node $\mathbf{v}_1$ are calculated by

$$\begin{pmatrix} u_{1,-1}^{q+1} \\ u_{2,-1}^{q+1} \\ u_{3,-1}^{q+1} \\ u_{4,-1}^{q+1} \\ u_{5,-1}^{q+1} \\ u_{6,-1}^{q+1} \end{pmatrix} = \frac{1}{3} \begin{bmatrix} 2 & -1 & -1 & -1 & -1 & -1 \\ -1 & 2 & -1 & -1 & -1 & -1 \\ -1 & -1 & 2 & -1 & -1 & -1 \\ -1 & -1 & -1 & 2 & -1 & -1 \\ -1 & -1 & -1 & -1 & 2 & -1 \\ -1 & -1 & -1 & -1 & -1 & 2 \end{bmatrix} \begin{pmatrix} u_{1,1}^{q} \\ u_{2,1}^{q} \\ u_{3,1}^{q} \\ u_{4,1}^{q} \\ u_{5,1}^{q} \\ u_{6,1}^{q} \end{pmatrix} \tag{A.1}$$

$$\begin{pmatrix} v_{1,-1}^{q+1} \\ v_{2,-1}^{q+1} \\ v_{3,-1}^{q+1} \\ v_{4,-1}^{q+1} \\ v_{5,-1}^{q+1} \\ v_{6,-1}^{q+1} \end{pmatrix} = \frac{1}{3} \begin{bmatrix} -2 & 1 & 1 & 1 & 1 & 1 \\ 1 & -2 & 1 & 1 & 1 & 1 \\ 1 & 1 & -2 & 1 & 1 & 1 \\ 1 & 1 & 1 & -2 & 1 & 1 \\ 1 & 1 & 1 & 1 & -2 & 1 \\ 1 & 1 & 1 & 1 & 1 & -2 \end{bmatrix} \begin{pmatrix} v_{1,1}^{q} \\ v_{2,1}^{q} \\ v_{3,1}^{q} \\ v_{4,1}^{q} \\ v_{5,1}^{q} \\ v_{6,1}^{q} \end{pmatrix} \tag{A.2}$$

The values of the ghost points around $\mathbf{v}_i$, $i = 2, \ldots, 7$ are calculated by

$$\begin{pmatrix} u_{i_1,m+1}^{q+1} \\ u_{i_2,m+1}^{q+1} \\ u_{i_3,-1}^{q+1} \\ u_{i_4,-1}^{q+1} \\ u_{i_5,-1}^{q+1} \\ u_{i_6,-1}^{q+1} \end{pmatrix} = \frac{1}{3} \begin{bmatrix} 2 & -1 & 1 & 1 & 1 & 1 \\ -1 & 2 & 1 & 1 & 1 & 1 \\ 1 & 1 & 2 & -1 & -1 & -1 \\ 1 & 1 & -1 & 2 & -1 & -1 \\ 1 & 1 & -1 & -1 & 2 & -1 \\ 1 & 1 & -1 & -1 & -1 & 2 \end{bmatrix} \begin{pmatrix} u_{i_1,m-1}^{q} \\ u_{i_2,m-1}^{q} \\ u_{i_3,1}^{q} \\ u_{i_4,1}^{q} \\ u_{i_5,1}^{q} \\ u_{i_6,1}^{q} \end{pmatrix} \tag{A.3}$$

$$\begin{pmatrix} v_{i_1,m+1}^{q+1} \\ v_{i_2,m+1}^{q+1} \\ v_{i_3,-1}^{q+1} \\ v_{i_4,-1}^{q+1} \\ v_{i_5,-1}^{q+1} \\ v_{i_6,-1}^{q+1} \end{pmatrix} = \frac{1}{3} \begin{bmatrix} -2 & 1 & 1 & 1 & 1 & 1 \\ 1 & -2 & 1 & 1 & 1 & 1 \\ 1 & 1 & -2 & 1 & 1 & 1 \\ 1 & 1 & 1 & -2 & 1 & 1 \\ 1 & 1 & 1 & 1 & -2 & 1 \\ 1 & 1 & 1 & 1 & 1 & -2 \end{bmatrix} \begin{pmatrix} v_{i_1,m-1}^{q} \\ v_{i_2,m-1}^{q} \\ v_{i_3,1}^{q} \\ v_{i_4,1}^{q} \\ v_{i_5,1}^{q} \\ v_{i_6,1}^{q} \end{pmatrix} \tag{A.4}$$

where the value of $(i_1, i_2, \ldots, i_6)$ is the same as Eq. (7).

The values of the ghost points for the fixed exterior nodes (without control) are calculated by

$$u_{k,m+1}^{q+1} = u_{k,m-1}^{q}, \qquad v_{k,m+1}^{q+1} = -v_{k,m-1}^{q} \tag{A.5}$$

The values of the ghost points for the exterior nodes which are applied with control law (17) and experiencing a disturbance force $f(t)$ (normalized) are calculated by

$$\begin{aligned} u_{k,m+1}^{q+1} &= \frac{(T_r^2 + c_r^2 K_r^2) u_{k,m-1}^{q} + 2c_r K_r T_r v_{k,m-1}^{q} - 2c_r T_r f^{q+1} + 2\Delta x (c_r K_r + T_r \alpha) \dot{f}^{q+1}}{c_r^2 K_r^2 - T_r^2}, \\ v_{k,m+1}^{q+1} &= \frac{-(T_r^2 + c_r^2 K_r^2) v_{k,m-1}^{q} - 2c_r K_r T_r u_{k,m-1}^{q} + 2c_r^2 K_r f^{q+1} - 2\Delta x (T_r + c_r K_r \alpha) \dot{f}^{q+1}}{c_r^2 K_r^2 - T_r^2}. \end{aligned} \tag{A.6}$$

where $K_r \neq T_r/c_r$, $\dot{f}$ is the derivative of f with respect to time t. When the exterior node under control experiences no disturbances, the values of the ghost points can be calculated by Eq. (A.6) with $f^{q+1} = \dot{f}^{q+1} = 0$. While when the exterior node without control experiences a force disturbance, the values of the ghost points can be calculated by Eq. (A.6) with $K_r = 0$.

Appendix B. Calculation of the total energy in the cable net structure by the trapezoidal rule

The energy of the kth string is

$$\mathbf{E}_{w^k}(t) = \frac{1}{2}\int_0^1 \left(\rho_k |w_t^k(t,x)|^2 + T_k |w_x^k(t,x)|^2\right) \mathrm{d}x. \tag{B.1}$$

where T_k and ρ_k are the normalized tension and the normalized linear density, respectively.

The space interval [0, 1] is discretized into m equally spaced panels for the string. By applying the trapezoidal rule to each panel, the approximation to the energy of this string (Eq. (B.1)) at time t_q becomes

$$\begin{aligned}
\mathbf{E}_{w^k}(t_q) &= \frac{1}{2}\sum_{p=0}^{m-1}\int_{p\Delta x}^{(p+1)\Delta x} \left(\rho_k |v^k(t_q,x)|^2 + T_k |c_k u^k(t_q,x)|^2\right) \mathrm{d}x \\
&= \frac{1}{2}\sum_{p=0}^{m-1} \frac{\rho_k}{2}\left[(|v_{k,p}^q|^2 + |u_{k,p}^q|^2) + (|v_{k,p+1}^q|^2 + |u_{k,p+1}^q|^2)\right]\Delta x \\
&= \frac{\rho_k}{4}\sum_{p=0}^{m-1}\left[(|v_{k,p}^q|^2 + |u_{k,p}^q|^2) + (|v_{k,p+1}^q|^2 + |u_{k,p+1}^q|^2)\right]\Delta x.
\end{aligned} \tag{B.2}$$

After a summation of $\mathbf{E}_{w^k}(t_q)$, we can obtain the total energy of the cable net structure at time t_q.

Appendix C. Supplementary data

Supplementary material related to this article can be found online at https://doi.org/10.1016/j.wavemoti.2017.11.004.

References

[1] M. Thomson, AstroMesh deployable reflectors for Ku and Ka band commercial satellites, in: 20th AIAA International Communication Satellite Systems Conference and Exhibit, Montreal, Quebec, Canada, 2002. http://dx.doi.org/10.2514/6.2002-2032.

[2] H. Hu, Q. Tian, W. Zhang, D. Jin, G. Hu, Y. Song, Nonlinear dynamics and control of large deployable space structures composed of trusses and meshes, Adv. Mech. 43 (4) (2013) 390–414.

[3] Y.R. Teo, A.J. Fleming, Optimal integral force feedback for active vibration control, J. Sound Vib. 356 (2015) 20–33. http://dx.doi.org/10.1016/j.jsv.2015.06.046.

[4] D.J. Inman, Vibration with Control, John Wiley & Sons, Ltd, 2006. http://dx.doi.org/10.1002/0470010533.

[5] M. Moshrefi-Torbati, J. Forrester, A. Forrester, A. Keane, M. Brennan, S. Elliott, Novel active and passive anti-vibration mountings, J. Sound Vib. 331 (7) (2012) 1532–1541. http://dx.doi.org/10.1016/j.jsv.2011.12.005.

[6] Y. Wu, W. Zhang, X. Meng, Y. Su, Nonlinear vibration control of cable net structures with bounded uncertainties, Acta Mech. 227 (10) (2016) 2985–3000. http://dx.doi.org/10.1007/s00707-016-1656-8.

[7] Z. Wang, T. Li, Optimal Piezoelectric sensor/actuator placement of cable net structures using H 2-norm measures, J. Vib. Control 20 (8) (2013) 1257–1268. http://dx.doi.org/10.1177/1077546312472927.

[8] L. Caracoglia, N. Jones, In-plane dynamic behavior of cable networks. part 1: formulation and basic solutions, J. Sound Vib. 279 (3–5) (2005) 969–991. http://dx.doi.org/10.1016/j.jsv.2003.11.058.

[9] J. Ahmad, S. Cheng, F. Ghrib, Impact of cross-tie design on the in-plane stiffness and local mode formation of cable networks on cable-stayed bridges, J. Sound Vib. 363 (2016) 141–155. http://dx.doi.org/10.1016/j.jsv.2015.09.052.

[10] M. Balas, Trends in large space structure control theory: Fondest hopes, wildest dreams, IEEE Trans. Autom. Control 27 (3) (1982) 522–535. http://dx.doi.org/10.1109/tac.1982.1102953.

[11] A.H. von Flotow, Traveling wave control for large spacecraft structures, J. Guid. Control Dyn. 9 (4) (1986) 462–468. http://dx.doi.org/10.2514/3.20133.

[12] T. Watanabe, P. Trivailo, W. Taira, H. Fujii, An analysis of vibration and wave-absorbing control of tether systems, in: AIAA Guidance, Navigation, and Control Conference and Exhibit, 2001. http://dx.doi.org/10.2514/6.2001-4033.

[13] N. Tanaka, Y. Kikushima, Active wave control of a flexible beam. proposition of the active sink method, JSME Int. J. III 34 (2) (1991) 159–167. http://dx.doi.org/10.1299/jsmec1988.34.159.

[14] Z. Wang, T. Li, Linear dynamic analysis and active control of space prestressed taut cable net structures using wave scattering method, Struct. Control Health Monit. 23 (4) (2015) 783–798. http://dx.doi.org/10.1002/stc.1810.

[15] Z. Shuang, Boundary Control of Flexible Mechanical Systems, National University of Singapore, 2012.

[16] C.H. Chung, C.A. Tan, Active vibration control of the axially moving string by wave cancellation, J. Vib. Acoust. 117 (1) (1995) 49. http://dx.doi.org/10.1115/1.2873866.

[17] H. Habibi, W. O'Connor, Wave-based control of planar motion of beam-like mass–spring arrays, Wave Motion 72 (2017) 317–330. http://dx.doi.org/10.1016/j.wavemoti.2017.04.002.

[18] E. Kreuzer, M. Steidl, Controlling torsional vibrations of drill strings via decomposition of traveling waves, Arch. Appl. Mech. 82 (4) (2012) 515–531. http://dx.doi.org/10.1007/s00419-011-0570-8.

[19] E. Rustighi, B. Mace, N. Ferguson, An adaptive anechoic termination for active vibration control, J. Vib. Control 17 (13) (2011) 2066–2078. http://dx.doi.org/10.1177/1077546311403788.
[20] A. Zingoni, An efficient computational scheme for the vibration analysis of high tension cable nets, J. Sound Vib. 189 (1) (1996) 55–79. http://dx.doi.org/10.1006/jsvi.1996.0005.
[21] A.H. Nayfeh, P.F. Pai, Linear and nonlinear structural mechanics, John Wiley & Sons, 2008. http://dx.doi.org/10.1002/9783527617562.
[22] G.F. Giaccu, L. Caracoglia, B. Barbiellini, Modeling "unilateral" response in the cross-ties of a cable network: Deterministic vibration, J. Sound Vib. 333 (19) (2014) 4427–4443. http://dx.doi.org/10.1016/j.jsv.2014.04.030.
[23] R. Claren, G. Diana, Mathematical analysis of transmission line vibration, IEEE Trans. Power Appar. Syst. PAS-88 (12) (1969) 1741–1771. http://dx.doi.org/10.1109/tpas.1969.292291.
[24] I. Vassilopoulou, C.J. Gantes, Vibration modes and natural frequencies of saddle form cable nets, Comput. Struct. 88 (1–2) (2010) 105–119. http://dx.doi.org/10.1016/j.compstruc.2009.07.002.
[25] L. Caracoglia, N. Jones, In-plane dynamic behavior of cable networks. part 2: prototype prediction and validation, J. Sound Vib. 279 (3–5) (2005) 993–1014. http://dx.doi.org/10.1016/j.jsv.2003.11.059.
[26] Y. Wu, W. Zhang, X. Meng, Y. Su, Compensated positive position feedback for active control of piezoelectric structures, J. Intell. Mater. Syst. Struct. (2017). http://dx.doi.org/10.1177/1045389x17708045. 1045389X1770804.
[27] G.Q. Xu, N.E. Mastorakis, Differential Equations on Metric Graph, Wseas Press, 2010.
[28] D.L. Russell, Controllability and stabilizability theory for linear partial differential equations: Recent progress and open questions, SIAM Rev. 20 (4) (1978) 639–739. http://dx.doi.org/10.1137/1020095.
[29] H. Sakamoto, K.C. Park, Y. Miyazaki, Distributed and localized active vibration isolation in membrane structures, J. Spacecr. Rockets 43 (5) (2006) 1107–1116. http://dx.doi.org/10.2514/1.20864.
[30] M. Aupérin, C. Dumoulin, G.E. Magonette, F. Marazzi, H. Frsterling, R. Bonefeld, A. Hooper, A.G. Jenner, Active control in civil engineering: From conception to full scale applications, J. Struct. Control 8 (2) (2001) 123–178. http://dx.doi.org/10.1002/stc.4300080201.
[31] P. Hagedorn, A. DasGupta, Vibrations and Waves in Continuous Mechanical Systems, John Wiley & Sons, Ltd, 2007. http://dx.doi.org/10.1002/9780470518434.
[32] R. Curtain, K. Morris, Transfer functions of distributed parameter systems: A tutorial, Automatica 45 (5) (2009) 1101–1116. http://dx.doi.org/10.1016/j.automatica.2009.01.008.
[33] E.I. Jury, A simplified stability criterion for linear discrete systems, Proc. IRE 50 (6) (1962) 1493–1500. http://dx.doi.org/10.1109/JRPROC.1962.288193.
[34] P.D. Lax, Weak solutions of nonlinear hyperbolic equations and their numerical computation, Commun. Pure Appl. Math. 7 (1) (1954) 159–193. http://dx.doi.org/10.1002/cpa.3160070112.
[35] J.W. Thomas, Numerical Partial Differential Equations: Finite Difference Methods, Springer Science & Business Media, New York, 2013.
[36] J.E. Lagnese, G. Leugering, E.J.P.G. Schmidt, Modeling, Analysis and Control of Dynamic Elastic Multi-Link Structures, Springer Science & Business Media, New York, 2012.
[37] L. Halpern, Absorbing boundary conditions for the discretization schemes of the one-dimensional wave equation, Math. Comp. 38 (158) (1982) 415. http://dx.doi.org/10.2307/2007278.
[38] R. Dáger, E. Zuazua, Wave Progagation, Observation and Control in 1-d Flexible Multi-Structures, Springer-Verlag, Berlin, 2006. http://dx.doi.org/10.1007/3-540-37726-3.
[39] Y. Zhang, G. Xu, Controller design for bush-type 1-d wave networks, ESAIM Control Optim. Calc. Var. 18 (1) (2012) 208–228. http://dx.doi.org/10.1051/cocv/2010050.